Ocean Dynamics (2018) 68:575–587
https://doi.org/10.1007/s10236-018-1149-5

Evaluation on surface current observing network of high frequency ground wave radars in the Gulf of Thailand

Xunqiang Yin [1,2,3] · Junqiang Shi [1,2,3] · Fangli Qiao [1,2,3]

Received: 31 October 2017 / Accepted: 21 March 2018 / Published online: 6 April 2018

Abstract

Due to the high cost of ocean observation system, the scientific design of observation network becomes much important. The current network of the high frequency radar system in the Gulf of Thailand has been studied using a three-dimensional coastal ocean model. At first, the observations from current radars have been assimilated into this coastal model and the forecast results have improved due to the data assimilation. But the results also show that further optimization of the observing network is necessary. And then, a series of experiments were carried out to assess the performance of the existing high frequency ground wave radar surface current observation system. The simulated surface current data in three regions were assimilated sequentially using an efficient ensemble Kalman filter data assimilation scheme. The experimental results showed that the coastal surface current observation system plays a positive role in improving the numerical simulation of the currents. Compared with the control experiment without assimilation, the simulation precision of surface and subsurface current had been improved after assimilated the surface currents observed at current networks. However, the improvement for three observing regions was quite different and current observing network in the Gulf of Thailand is not effective and a further optimization is required. Based on these evaluations, a manual scheme has been designed by discarding the redundant and inefficient locations and adding new stations where the performance after data assimilation is still low. For comparison, an objective scheme based on the idea of data assimilation has been obtained. Results show that all the two schemes of observing network perform better than the original network and optimal scheme-based data assimilation is much superior to the manual scheme that based on the evaluation of original observing network in the Gulf of Thailand. The distributions of the optimal network of radars could be a useful guidance for future design of observing system in this region.

Keywords Gulf of Thailand · High frequency radar · Observation system simulation experiment · Surface current

1 Background

As one of the ten largest Gulfs in the world, the Gulf of Thailand is located in the south-east of South China Sea with abundant fishery resources and rich in petroleum resources. There are many natural disasters happened in this region, such as monsoonal flood (Saramul and Ezer 2014) and severe storm surge (Tomkratoke et al. 2015). But the observing networks in hydrology are quite limited and starting very late. Due to the lack of information and effective prevention and alert, surrounding countries suffered a lot of lost on the aquaculture and agriculture near the coast. Since 2012, the Geo-Informatics and Space Technology Development Agency of Thailand has developed a project (http://coastalradar.gistda.or.th/) of the coastal radar warning system for the land and the sea, aimed to manage the tides and waves in the coast region. Until 2016, an array of high frequency ground wave radars was ready and the surface currents near the coast could be obtained operationally. The radar stations are mainly located in three regions (Fig. 1). In the upper of the Gulf (UG), there are 7 radars (CHAM, PHET, SASO, SASA, SAPA, LAMT, and PATT) to observe the surface currents around the Gulf of

Responsible Editor: Tal Ezer

This article is part of the Topical Collection on the *9th International Workshop on Modeling the Ocean (IWMO), Seoul, Korea, 3–6 July 2017*

✉ Xunqiang Yin
yinxq@fio.org.cn

[1] The First Institute of Oceanography, State Oceanic Administration, Qingdao 266061, China

[2] Laboratory for Regional Oceanography and Numerical Modeling, Qingdao National Laboratory for Marine Science and Technology, Qingdao 266237, China

[3] Key Lab of Marine Science and Numerical Modeling, SOA, Qingdao 266061, China

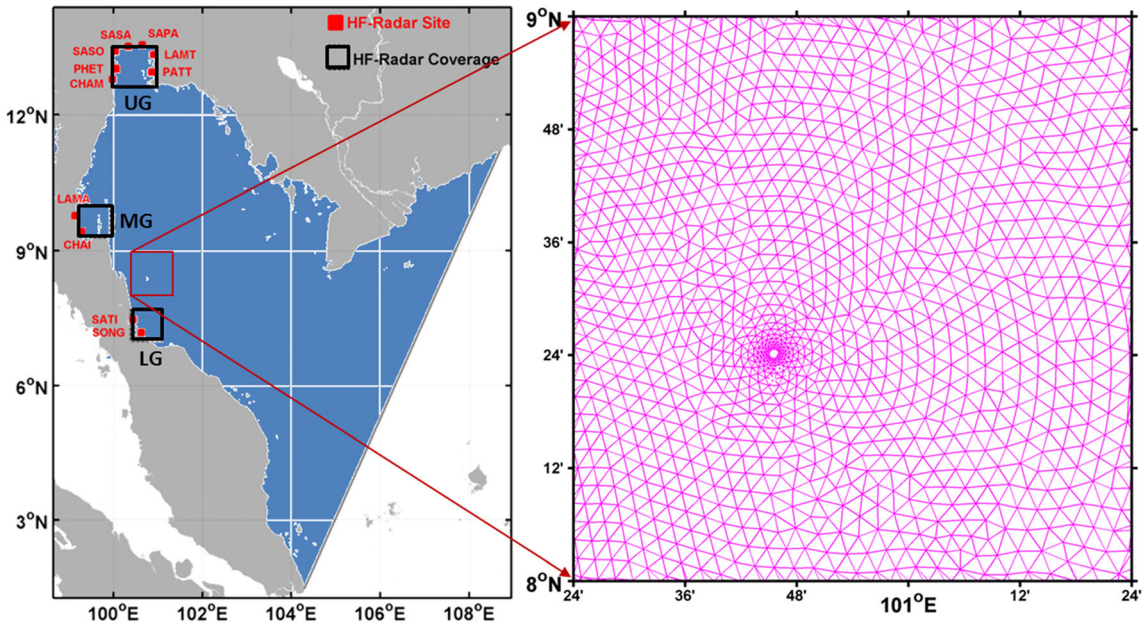

Fig. 1 Distributions of the high frequency ground wave radars and model domain (blue area) for the Gulf of Thailand. Red dots represent the location of high frequency ground wave radar stations, and these radar stations have been divided into three regions as shown by the black boxes named UG, MG, and LG. The triangle grids of the model in the red box are provided in the right panel

Bangkok. And there are 2 radars (LAMA and CHAI) in the middle Gulf (MG) along the west coast and 2 radars (SATI and SONG) in the lower Gulf (LG) along the west coast. These radars could observe radial velocity at the sea surface; not less than 2 radars should work together to get the vector of surface currents. These radars will observe every hour and covers about 70 km. The observed sea surface currents are potentially helpful to provide the status of the sea in near real time and the observed data could be assimilated into coastal ocean model to improve the forecast skills in this region. Numerical experiments are required to evaluate the performance of current observing network. Furthermore, if new observing resources are available, how to add more stations is another question need to be studied based on numerical experiments.

If more stations are available to observe the Gulf of Thailand, it will be definitely helpful to the related forecast and the alert of marine disasters, while the cost of the observing system will also become larger. How to design the observing network with a limited financial support to provide more efficient information is a very important topic. In traditional research of the oceanography, the design of observing network is based on the knowledge obtained from history observations in the studied region. More practical way to determine the observing locations could be based on where the forecast skills are relatively low. In recent years, there are many studies focused on observing system simulation experiments (OSSEs) using the data assimilation ideas to investigate the potential impacts of prospective observing systems (Masutani et al. 2010) and provide optimized designing of the observing network. There are two kinds of method for observing network optimization in literatures. One is based on the variational data assimilation method to find the area where the initial errors will grow quickly (Buizza et al. 1995; Palmer et al. 1994, 1998; Gelaro et al. 1999), or find the regions with bigger gradient of the cost function aspect to the initial conditions (Bergot et al. 1999; Langland et al. 1999; Baker and Daley 2000). The other kind is the ensemble-based methods (Morss et al. 2001; Bishop and Toth 1999; Bishop et al. 2001) to find where to do the observation will reduce the forecast errors more significantly.

The OSSEs have been applied to evaluate (optimal design) the observing network in many regions, especially for some worldwide projects. For example, She et al. (2007) employed OSSEs to evaluate the observing networks of sea surface temperature in the Baltic Sea and North Sea, and multi-indicator approaches including data quality, effective data coverage, field reconstruction error, and model nowcast error have been used for evaluation. Sakov and Oke (2008) discussed the objective array design for the tropical Indian Ocean based on the Kalman filter theory. In order to design optimal monitoring network in the coastal ocean, Xue et al. (2011) performed the OSSEs with ensemble Kalman filter in Nantucket Sound, Massachusetts. Peng et al. (2016) employed a set of OSSEs that evaluate the performance of a three-dimensional variational data assimilation (3DVAR) system based on the Regional Ocean Modeling System (ROMS) for South China Sea, and the impacts of different types of observations have been investigated.

This work aims to evaluate the observing network of the high frequency grand wave radars in the Gulf of Thailand and

provide some advice on how to optimize the future network for this region. The flowchart of this work is given in Fig. 2. In Section 2, a coastal ocean model and the related data assimilation will be designed for the Gulf of Thailand, and a forecast experiment based on the observed surface currents will be tested. In Section 3, some experiments will be carried out to evaluate the performance of current observing network. In Section 4, a manual design of the observing network based on the evaluation results and an objective design based on ensemble Kalman filter have been compared. And Section 5 is the summary and discussion.

2 Ocean forecast system of the Gulf of Thailand

2.1 Regional ocean model of the Gulf of Thailand

Considering that the coast line of the Gulf of Thailand is quite complex and there are many islands in this region, the Finite Volume Coastal Ocean Model (FVCOM, Chen et al. 2006) is employed to setup the three-dimensional coastal ocean model in this study. The model domain is shown in Fig. 1. The unstructured triangle grids are used and the local mesh refinement is performed for the near shore and islands. The smallest grid size is about 330 m and the grid size on average is about 3300 m. At the open boundary, the grid size is about 1000 m. There are 21 layers in vertical direction. The model topography is interpolated from the 30 arc sec spatial resolution GEBCO (General Bathymetric Chart of the Oceans) bathymetry (Weatherall et al. 2015) and the observation of water depth provided by Phuket Marine Biological Center (PMBC) in the near-shore region has been merged to the interpolation results.

At the open boundary, eight main tidal constituents (M2, S2, N2, K2, K1, O1, P1, and Q1) have been considered and the sea level at the open boundary is calculated using the harmonic constants of these tidal constituents (Pawlowicz et al. 2002). The currents, temperature, and salinity at the boundary are interpolated from the results of an assimilated global circulation model of FIOCOM (wave-tide-circulation coupled ocean model developed by the first institute of oceanography, state oceanic administration of China) with the horizontal resolution of 0.1°. In this global model, the ensemble adjustment Kalman filter was used to assimilate the sea surface temperature (SST), sea level anomaly (SLA), and Argo temperature/salinity profiles (Yin et al. 2011), and the results are more reliable (Shi et al. 2018) compared with other observations. To reduce the noise due to the boundary reflections, the sponge layer has been used at the open boundary. The monthly runoff amount of Mekong River and Chao Phraya River provided by PMBC is used as land input for this model.

The initial condition of this model was zero flow and a flat sea surface. The initial value of temperature and salinity are interpolated from the assimilation results of the FIOCOM. The surface forcing of this model includes the wind interpolated from gridded surface vector winds of CCMP (Cross-Calibrated Multi-Platform) V2.0 provided by Remote Sensing Systems (Atlas et al. 2009, 2011; Scott et al. 2016), the short wave radiation, sensible heat flux, and latent heat flux interpolated from the Climate Forecast System Reforecast version 2 (CFSv2, Saha et al. 2012). In Wu et al. (2015), the co-tidal charts for M2, S2, K1, and O1 have been provided and discussed which shows that the tide is a key process in the Gulf of Thailand. These distributions from this model are given in Fig. 3 and they agree with previous studies. The model

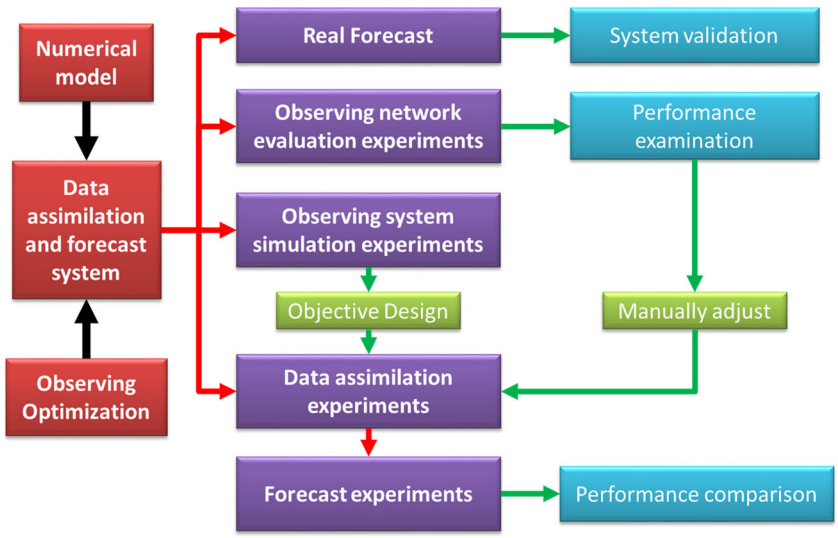

Fig. 2 Flowchart of this work

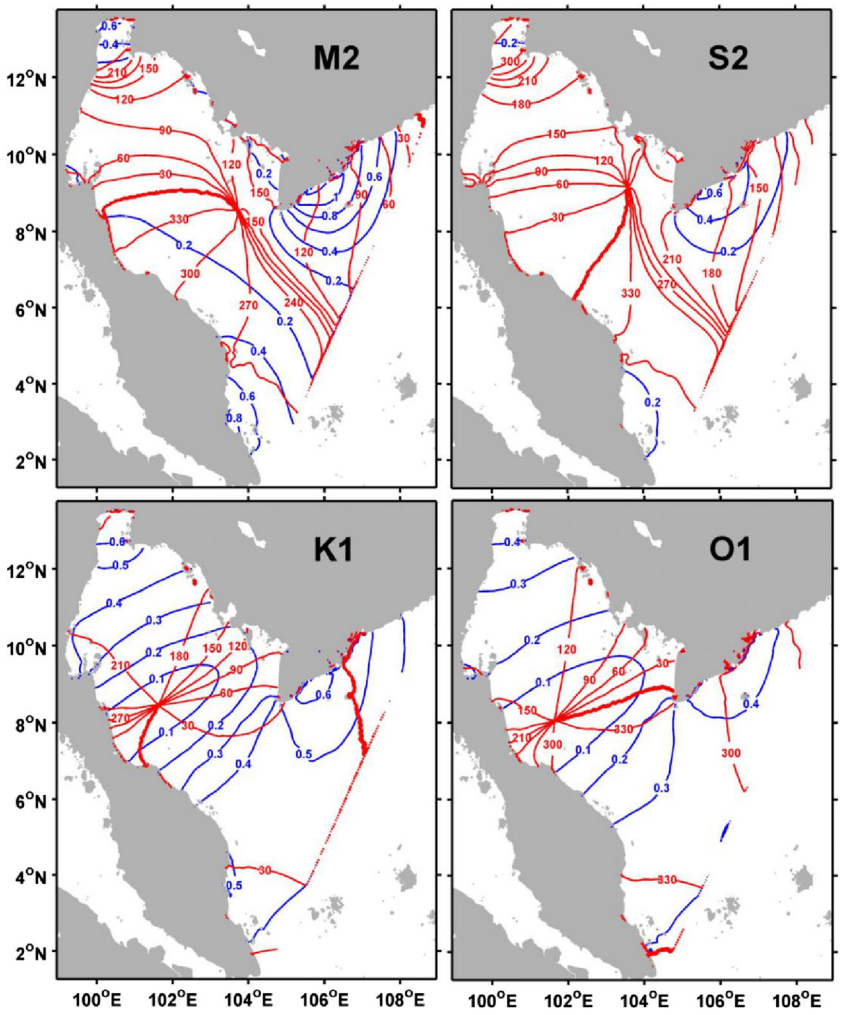

Fig. 3 Predicted co-tidal chart for M2, S2, K1, and O1. Red line is the phase and blue line is the amplitude

built in this section will be used to evaluate the current observing network in the following sections.

2.2 Data assimilation scheme

An improved ensemble Kalman filter based on the Canadian Quick Covariance method (CQC, Jackson et al. 2008) and the static sampling method (Sun et al. 2017) have been employed to do the data assimilation of surface currents observed by high frequency ground wave radar. Different with the traditional ensemble Kalman filter (EnKF, Evensen 1994), the forecast errors were reconstructed by the trend of forecast and the ensemble running of the forecast model is not required. Once the forecast model finished one run, the model output can be used to construct the ensemble members at each assimilation time (Fig. 4).

The ensemble sample is constructed by the difference between a fixed time of interval forecasts. Given the previous output of the forecast which is $\{A^{t_0-i\Delta}, i = 0, L\ , N\}$, the i-th sample of the model background error with zero ensemble mean can be expressed as

$$A_i^{'} = \left(A^{t_0-i\Delta} - A^{t_0-(i-1)\Delta}\right) - \left(A^{t_0-N\Delta} - A^{t_0}\right)/N$$

where N is the ensemble size, Δ is the time interval of the output, and t_0 is the last time of the output. Then, the i-th ensemble member at time t can be constructed as

$$A_i^{'} = A^t + a\left[\left(A^{t_0-i\Delta} - A^{t_0-(i-1)\Delta}\right) - \left(A^{t_0-N\Delta} - A^{t_0}\right)/N\right]$$

Here, the factor α can be used to modify the ensemble spread and its value could be determined by the comparison of the constructed samples against the model errors between model results and observations.

In this formula, if $t_0 = t$, it is the dynamic sampling method in Sun et al. (2017) and the constructed background errors will be updated over time; otherwise, it will be the static sampling method. In this study, the static sampling method is used and the time interval is set to 1 h to focus on the tidal processes in

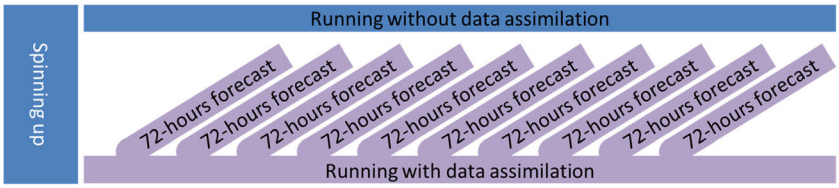

Fig. 4 Forecast experiments for the Gulf of Thailand. The spinning up is from May 27 to 31, 2016, and the data assimilation of the surface currents observed by high frequency ground wave radar is started at 00 UTC June 1, 2016. The observations have been assimilated by 6 h and the 72-h forecasts are carried out at 00 UTC of each day. The forecast results are output by hourly for comparison

this coastal region. Based on this ensemble, the model states could be updated similar as the EnKF (Evensen 2004).

2.3 Forecast experiments

Two experiments have been designed using the coastal model for the Gulf of Thailand, one without data assimilation which is a free run of this model and the other experiment with the data assimilation of hourly surface current observed by high frequency ground wave radar for better initial condition. The Gulf of Thailand model is started on May 27, 2016, for few days spinning up before these experiments started since 00 UTC in June 1. The observations used to do data assimilation are from June 1 to June 30, 2016. As shown in Fig. 5, the experiment of free run without data assimilation is carried out for comparison and the forecasts are started at 00 UTC of each day since June 1. In the forecast experiments, the data assimilation is carried out to prepare the initial conditions of the forecast. The observations have been assimilated every 6 h, that is the observation at 00, 06, 12, and 18 UTC has been sequentially assimilated into the model.

The model results of the free run and the forecast of 24, 48, and 72 h were compared with the observations of surface currents. The root mean square errors (RMSE) of the surface currents between model simulation and observations were given in Fig. 5. The time-averaged RMSE of the free run without data assimilation are 10.6 cm/s for U (x-component) and 10.7 cm/s for V (y-component). Since the observation of surface currents has been assimilated into the initial conditions, the errors in the forecast results have been reduced compared to the one from the free run. The reduction of the RMSE in the forecast of 24, 48, and 72 h is 7.7, 3.3, and 1.4% for U and they are 14.0, 4.8, and 1.6% for V. The error in the forecasts is increasing according to the forecast period and the influence due to the initial condition is reducing along time.

The snap distributions of the surface currents of the model free run, observation, and 24-h forecast are given in Fig. 6. It shows that the simulations have an obvious difference with the observation. The directions of surface currents from the free run model are mainly southern ward while the observations are mostly directly to south-east. In the southern part of this region, the simulated surface currents are larger than observation. The 24-h forecast results are closer to the observation because the data assimilation improved the initial conditions. This figure also shows that there are still a lot of differences between the forecast and observations and the observations used to improve the initial condition of the forecast may not be sufficient. These results indicated that this forecast system could join the coastal ocean model and the surface currents observed by the high frequency ground wave radar to improve the forecast results. But how to add new observations or adjust the observing network to significantly improve the forecast results needs to be studied further.

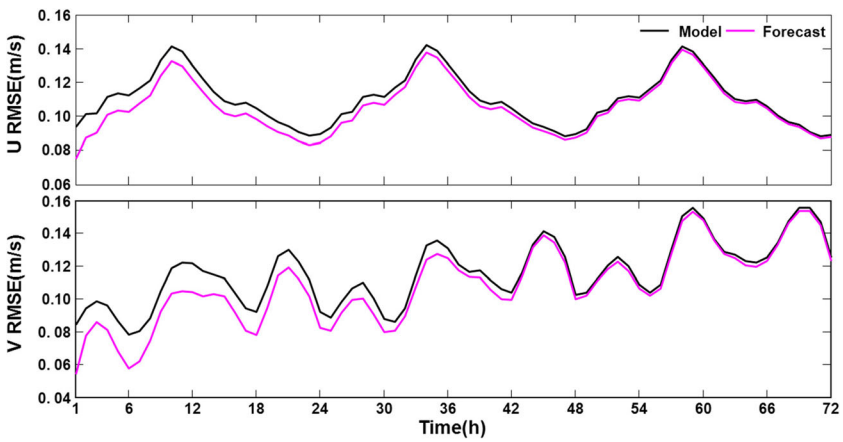

Fig. 5 The RMSE in U (upper) and V (lower) of the forecast (pink) and free run (black) experiments for the Gulf of Thailand as a function of the forecast leading time

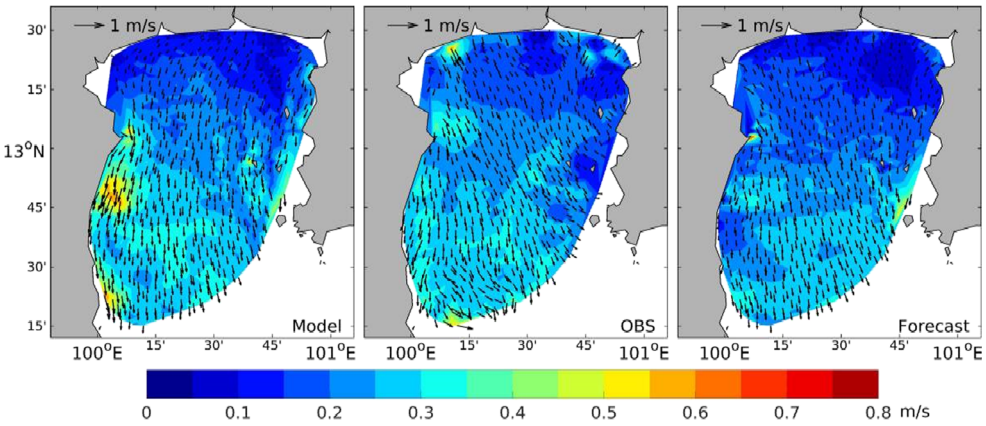

Fig. 6 The surface currents of the model free run (left), observation (middle), and 24-h forecast (right). The arrows are the surface current and filled color is for the speed

3 Evaluation of current observing network

3.1 Designing of experiments

In order to evaluate the current observing network, a set of experiments have been designed. Since the observations are divided into three regions (Fig. 2), these are not enough to evaluate the overall performance of the data assimilation in this domain. Following the typical way used in the study of OSSEs (Michiko et al. 2010), the model in Section 2 has been used as a perfect model to provide the "truth" for all the grid points along the experiment period. The observations used for data assimilation are obtained by adding noise to the "truth" and the locations of the observations are the same as the current observing network. The "observations" of sea surface currents in UG, MG, and LG regions have been generated for the data assimilation in this section and all the model results from the "truth" run have been used to do the related comparison.

To make the model results different with the "truth," the settings of this model have been changed to setup the control run experiment (CTL) without data assimilation. There are two mainly different settings have been used for CTL. One is the topography which is generated only by the GEBCO data set and the in situ observations of water depth are not used. The other difference is the heat flux at sea surface that has been replaced to the NCEP reanalysis 1 (Kalnay et al. 1996). As a result, the difference of surface currents between the CTL and the "truth" run is about 0.1 m/s on average.

Based on the model of CTL, seven assimilation experiments have been carried out and observations in different regions have been assimilated in different experiments for comparison. The assimilation experiments have been named by the regions where the observations have been assimilated. There are three experiments (UG, LG, and MG) that only the observations in one region have been assimilated. There are also three experiments in which the observations in two regions have been assimilated and they are named as UGMG, MGLG, and UGLG. The rest one is named as UGMGLG in which the observations in all these three regions have been assimilated. The period of the CTL and assimilation experiments is 1 month from January 6 to February 6, 2015.

3.2 Results

The RMSE between the simulation and the "truth" are calculated for all the experiments. The time series of these RMSE (Fig. 7) shows that the errors after data assimilation are all reduced significantly. For the experiments that only the observations in one region have been assimilated, the error reductions are quite different. The experiment MG has the biggest error reduction and the experiment LG is the smallest. This means that the observations in the MG region are more efficient than the others to improve the simulation in the whole domain. After the observations in two regions have been assimilated, the error reduction is completely greater than those only assimilating the observations in one region. Within these three experiments assimilating observations in two regions, the smallest error reduction is the MGLG and the other two experiments (UGLG and UGMG) are quite similar. Among all the experiments, the OSE3 with the observations in three regions which have been assimilated has the biggest error reduction. It is worth to be mentioned that the performance of UGLG and UGMG is quite similar to the UGMGLG. It means that the observations in regions MG and LG have similar contribution to improving the simulation results. To clearly show these differences, Fig. 8 gives the percentage of the error reduction of U and V. The difference shown in Fig. 7 can be seen obviously and it also shows that the UGLG has a slightly bigger error reduction than the UGMG.

The special distributions of the error reductions are given in Figs. 9 and 10. For the experiments that only the observations in one region have been assimilated, the error reductions are mainly around the observing locations. For those experiments that the observations in two regions have been assimilated, the coverage of high error reductions is not only around the

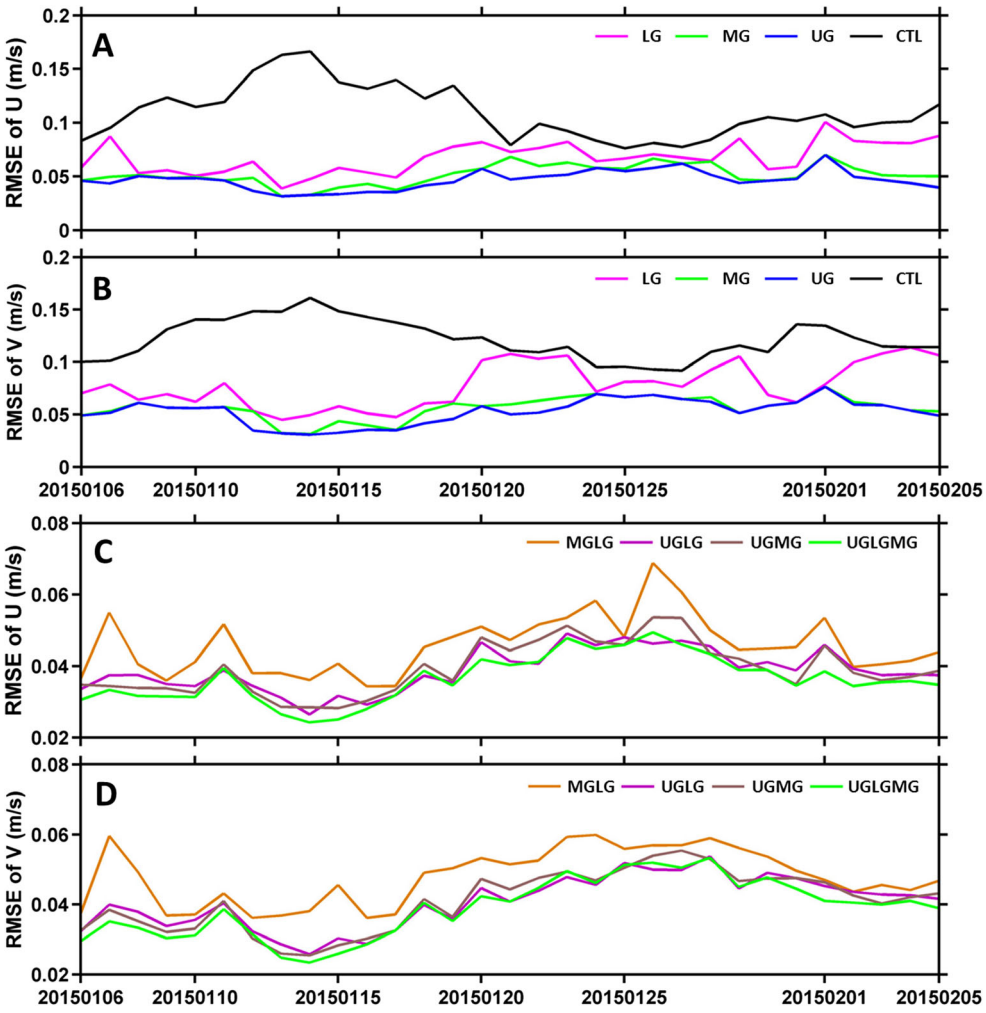

Fig. 7 Time serial of the RMSE in experiments of CTL and assimilation experiments. The regions for observations assimilated in each experiment are marked under their legend. The RMSE of U and V from the experiments LG, MG, UG, and CTL are given in panels **a** and **b**, and the RMSE of U and V from the experiments MGLG, UGLG, UGMG, and UGLGMG are given in panels **c** and **d**

observing locations. This means that the joint observing in different locations is much important than that in one location. The observing network could be determined by examining the distribution of the error reduction. Even the error reduction in UGMGLG has the biggest coverage in spatial, there are still many locations where the error reductions are quite smaller. More observations in other locations are required for further improving the simulation in these locations and the adjustment of the current observing network is necessary to make them more efficient.

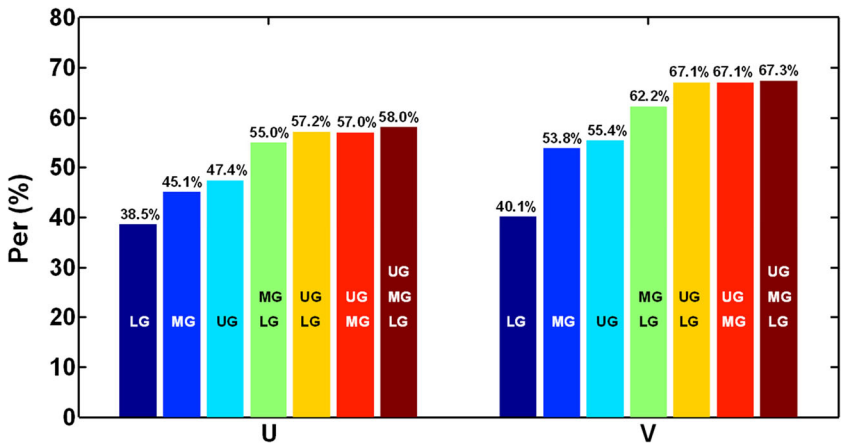

Fig. 8 Reduction percentage of the RMSE in the surface currents from assimilation experiments relative to CTL without data assimilation

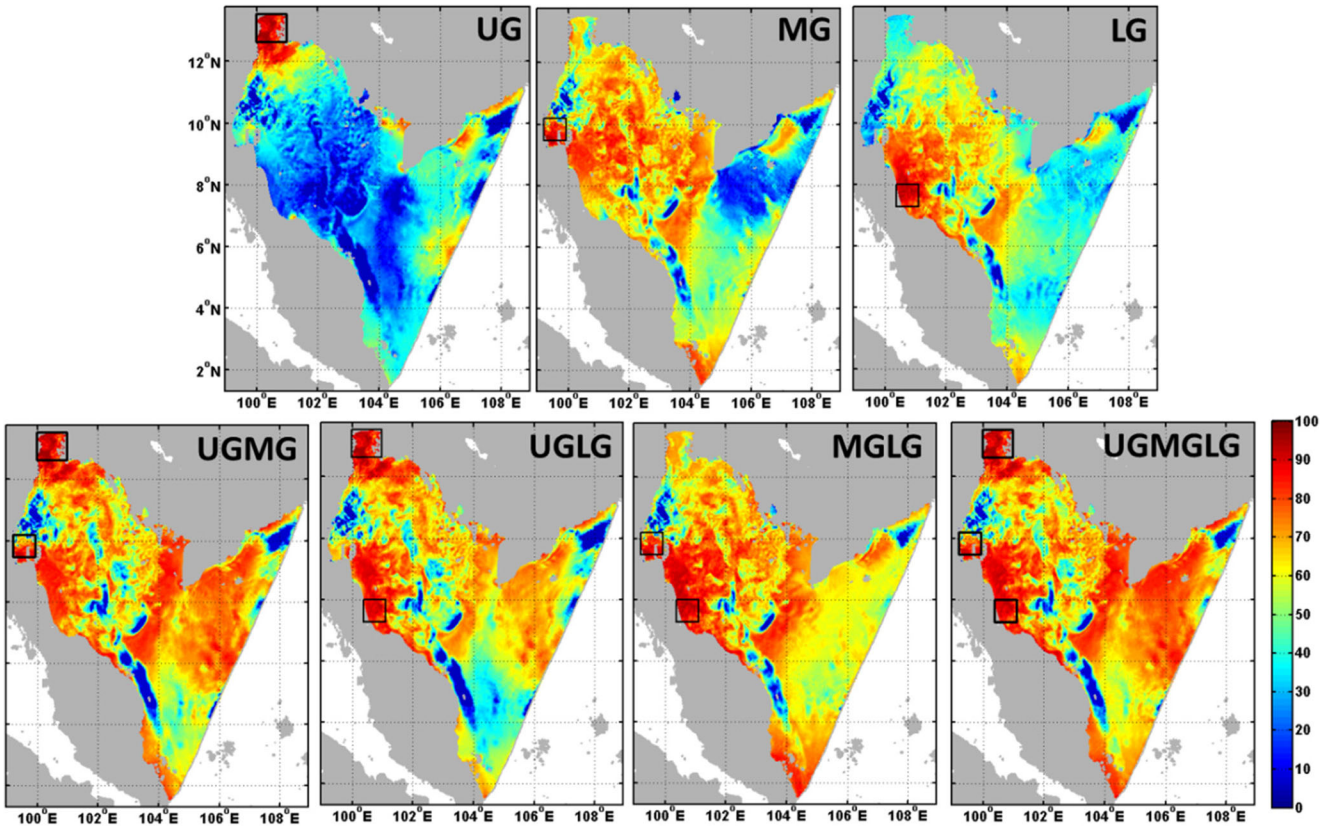

Fig. 9 Spatial distribution of the RMSE reduction percentage for U component from assimilation experiments relative to the CTL without data assimilation. The coverage regions of radars are marked by black boxes and the name of assimilation experiments have been shown in the upright corner of each panel

4 Optimal designing of the observing network

The evaluation of the current observing network shows that if only two regions (UG and MG, or UG and LG) left to observe the surface currents, the assimilation performance will be quite similar to the one that uses all the observations from three regions. Furthermore, if only one region provides observations of surface current to do assimilation, the observations in UG and MG regions perform super to the LG region. The observation in LG region could be removed for the update observing network. For those regions where the error reductions are relatively smaller in Figs. 9 and 10, more observing locations are required. Then, a manual optimization of the observing network (left panel in Fig. 11, hereafter refer to OPT1) can be obtained based on this evaluation. The original LG region has been removed and four new regions (N1, N2, N3, and N4) have been added. The high frequency ground wave radars in original regions have not changed and 2 radars have been put at each new region. Finally, there are a total of 17 radars in the new observing network. The optimal method for OPT1 is typically and directly used where the errors in the forecast results are still large. In most cases, these errors may not be generated locally but caused by the initial errors in other locations. An objective method based on the idea of data assimilation will be used to optimize the observing network for a better performance.

In the framework of EnKF, the ensemble states have been used to calculate background error covariance matrix (P^b) and it represents the uncertainties of model. Then, the analysis error covariance matrix (P^a) will be obtained after the observations have been assimilated. In this context, the optimized observing locations can be defined as the minimization of the analysis error covariance matrix. Considering the trace of the normalized analysis error covariance to represent the system error covariance (Sakov and Oke 2008), the optimal observation matrix can be given as follows:

$$H^{\mathrm{opt}} = \underset{\{H\}}{\arg\max}\left(\|P^a\|\right) = \underset{\{H\}}{\arg\max}\left[\mathrm{trace}\left(\frac{HP^b\left(HP^b\right)}{HP^bH^T + R_H}\right)\right]$$

where H represents the observing operator which could be used to transfer the states in model grid into observation locations, trace () means the triangle elements of the matrix, $\arg\min_{\{H\}}$ / $\arg\max_{\{H\}}$ is the operator to find the optimal H which will minimize/maximize the value, R_H is the error covariance of observations, and H^{opt} is the optimal H.

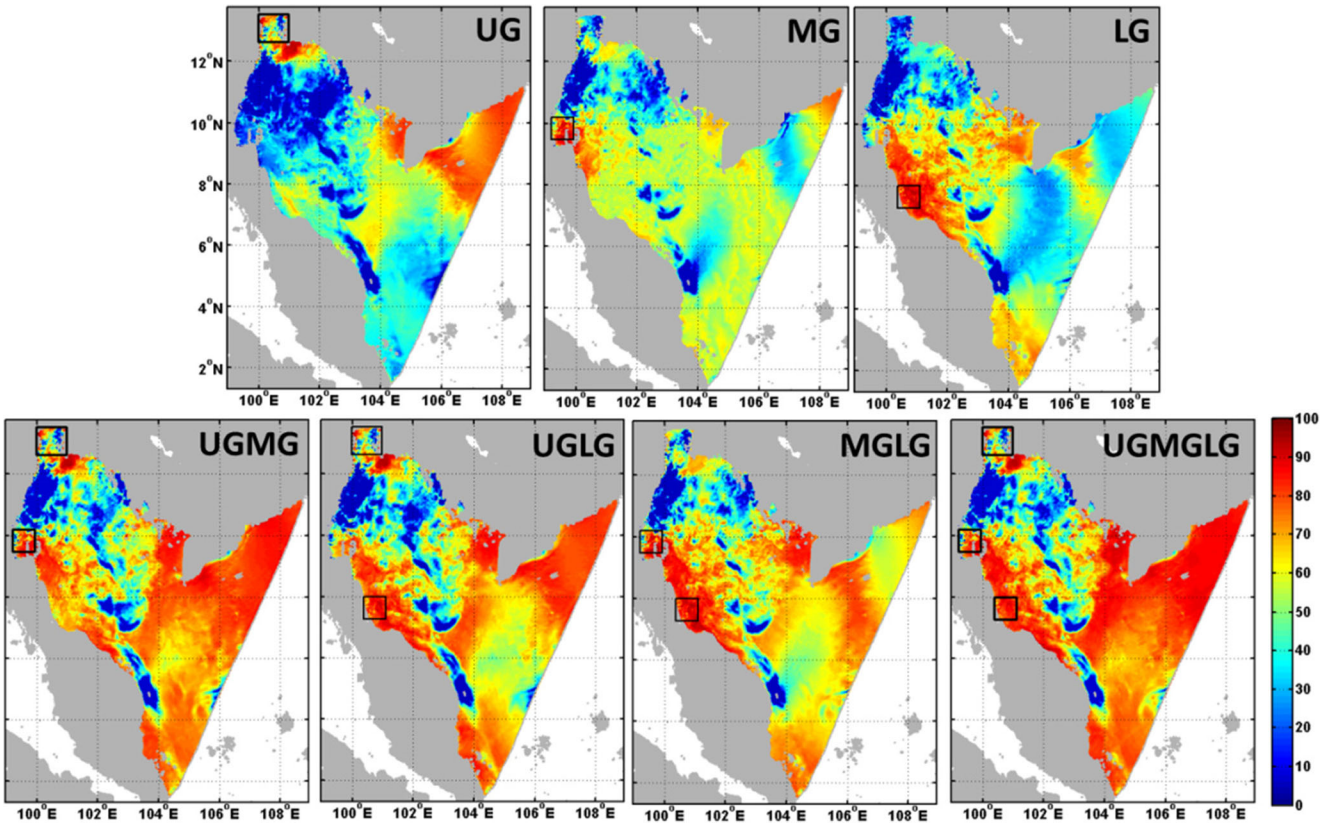

Fig. 10 Same as Fig. 8 but for V component

In order to simplify the calculation, only one observing location has been applied. The above formula can be simplified to

$$l = \underset{i=1,L,N}{\arg\max} \left[\frac{1}{P_{ii}^{b} + r(i)} \sum_{j=1}^{N} \left(P_{ij}^{b} \right)^{2} \right]$$

Here, arg $\max_{i=1,L,N}$ means the maximization process to find an optimal i, N is the number of observations, and P_{ii}^{b} and $r(i)$ are the elements of P^{b} and R_H respectively.

Applying this formula to all the grid point, the first optimal observing location could be obtained. After the observations in this optimal location have been assimilated, the ensemble states will be updated. Then, based on the updated (analysis)

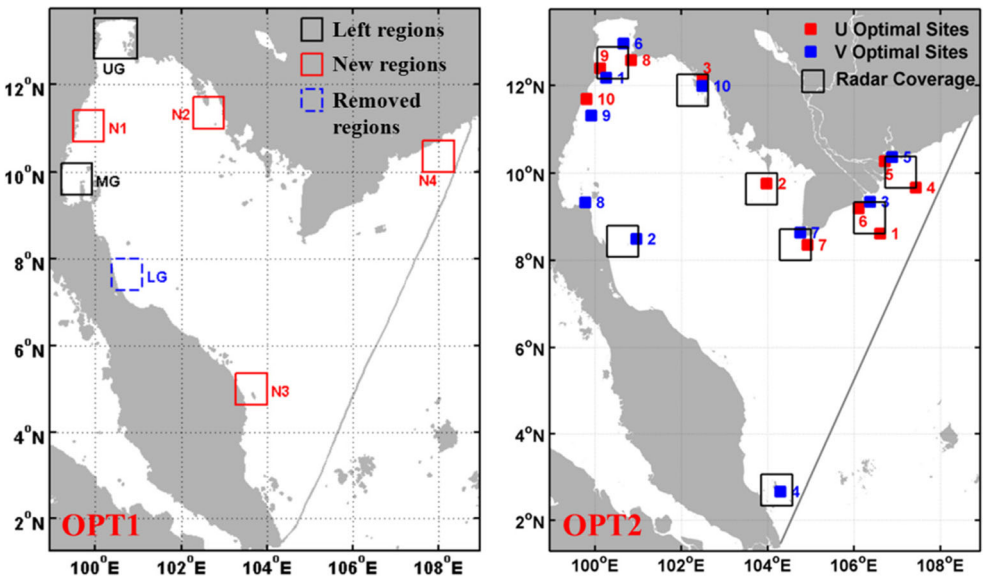

Fig. 11 Optimized observing locations of high frequency ground wave radars. Left is the manual scheme based on the evaluation of original radar networks and right is the objective scheme-based data assimilation idea

ensemble states, the next optimal location will be found by repeating the above steps.

This optimal method is used to find the optimal locations observing surface currents in the Gulf of Thailand. The first 20 stations have been obtained for U and V respectively. But there are some stations far from the land and they are not possible to be observed by the high frequency ground wave radar. The final stations have been selected according to the distance to land. Based on the distribution of these stations, eight regions (black boxes in the right panel of Fig. 11, hereafter refer to OPT2) have been selected to put radars to observe the surface currents. In order to use the similar numbers of radars with the manually optimization method, 2 radars have been put at each region and the total number in this scheme is 16. The main difference of the stations between two schemes is that more stations in the west of the domain are required in OPT1 while more radar stations in the east of the domain are required in OPT2.

The performance of these two schemes has been examined by the assimilation and forecast experiments. At the regions covered by the radars from two schemes, the "observations" of surface currents have been prepared using the same way as in Section 3. Two observing system simulation experiments (OPT1 and OPT2) have been designed to assimilate the surface currents from two schemes respectively. At 00 UTC of each day, the 72-h forecast has been started for further comparison.

The horizontal distributions of RMSE in two experiments have been given in Fig. 12. This is the comparison of history run after data assimilation against with the "truth." In most region of the model domain, the error reductions from two experiments are more than 80%. The results of OPT2 are obviously better than OPT1. Compared with the results in Figs. 9 and 10, observation at four new regions will increase the error reduction for the whole domain, but the improvement around these four regions is not much. The selected observing regions by manual scheme may not be reasonable. While in OPT2, the error reductions at the observing regions are quite clear. The model dynamics have been considered in OPT2 during the optimization based on the idea of data assimilation; the observing network could induce more improvement for the simulation at the whole domain and the observing locations.

And then, the vertical structures of error reductions have been compared in Fig. 13. The RMSE of the CTL without any data assimilation in vertical are about 5–8 cm/s for U and 5–

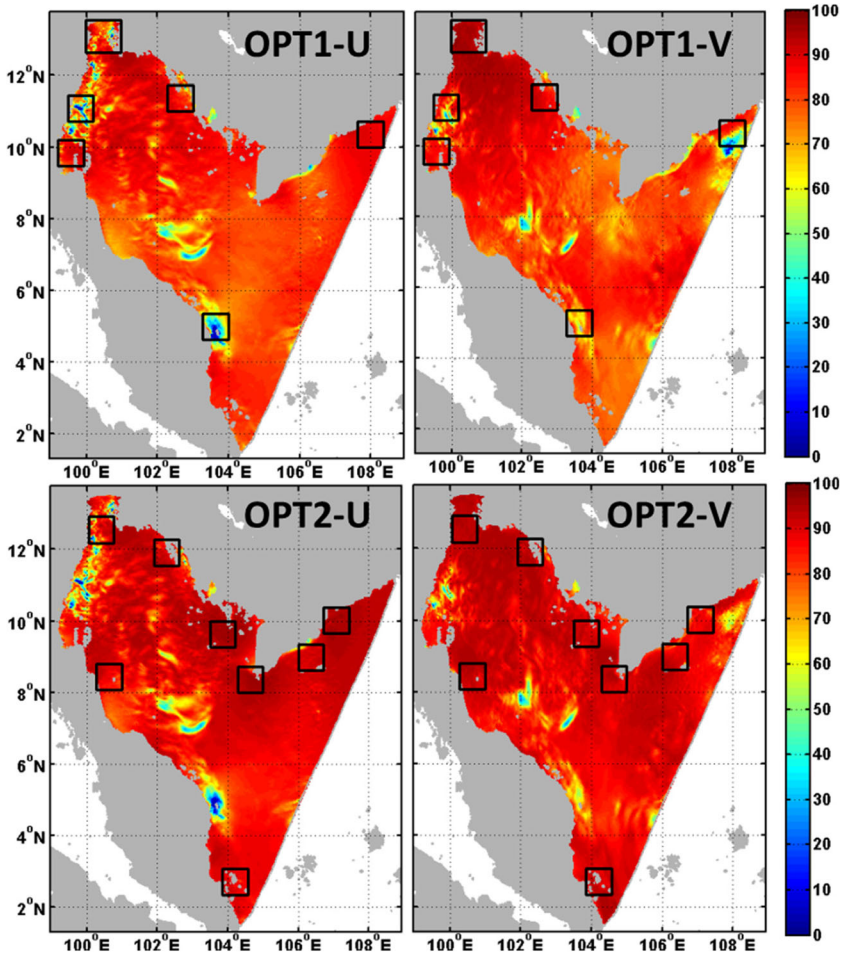

Fig. 12 Horizontal distribution of the RMSE reduction percentage in U (right) and V (left) after assimilated observations at locations of OPT1 (upper) and OPT2 (lower)

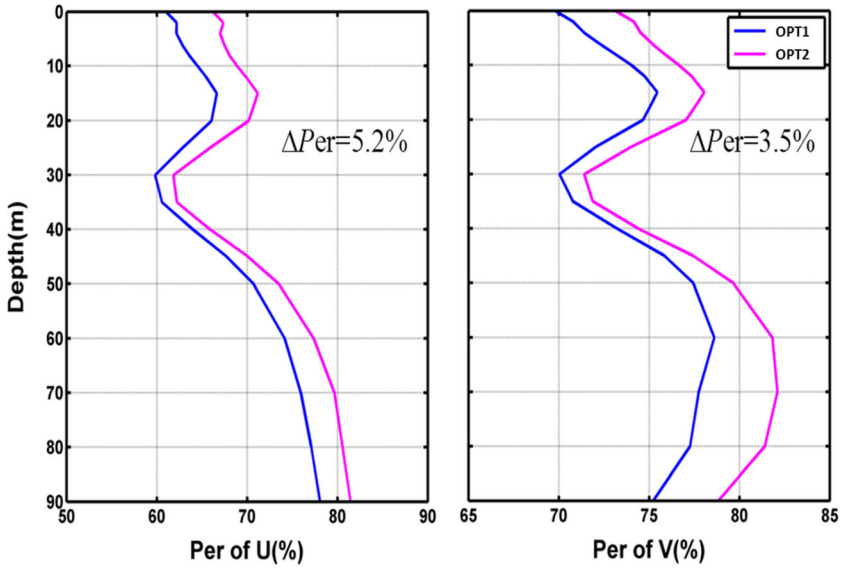

Fig. 13 The RMSE reduction percentage in U (left) and V (right) along vertical for experiments after assimilated observations at locations of OPT1 (blue) and OPT2 (pink)

13 cm/s for V. For both of the two assimilation experiments, the error reductions of U and V due to data assimilation are more than 60 and 70% respectively. The improvement of V component of two experiments is much higher than that of U. The error reductions around the depth of 30 m are relatively smaller than the other layers. Overall, the result of the OPT2 is much better than the OPT1 and there are more error reductions of 5.2 and 3.5% in U and V respectively.

The RMSE between the forecast and the "truth" results have been calculated as a function of the forecast leading time (Fig. 14). Within 72 h, the forecast results of two experiments are all significantly smaller than the CTL. That means the observations of surface currents using both the optimized schemes are all efficient to improve the forecast results. For the 24-h forecast, the error reduction of the forecasted U (V) compared with the CTL is 9.3% (13.3%) in OPT1 and 12.2% (16.3%) in OPT2. But for 48-h forecast, the error reduction becomes smaller which is 4.3% (6.7%) in OPT1 and 5.5% (8.4%) in OPT2. And for the 72-h forecast, the error reduction becomes even smaller which is 3.9% (5.8%) in OPT1 and 5.1% (7.2%) in OPT2. Similarly, the effects of the data assimilation in short period of forecast are more significant than longer forecast. The forecast errors of OPT2 are smaller than that of the OPT1 at all the forecast period.

All these experiments show that observations using two schemes will improve the simulation and forecast results. The error reductions in horizontal space and vertical depth due to data assimilation have been analyzed. The errors of forecast results were also provided for further comparison. All these comparisons indicate that the scheme based on data assimilation shows a better performance.

5 Summary and discussion

In order to evaluate the current observing network of the high frequency ground wave radars in the Gulf of Thailand, a serial of numerical experiments has been carried out in this study.

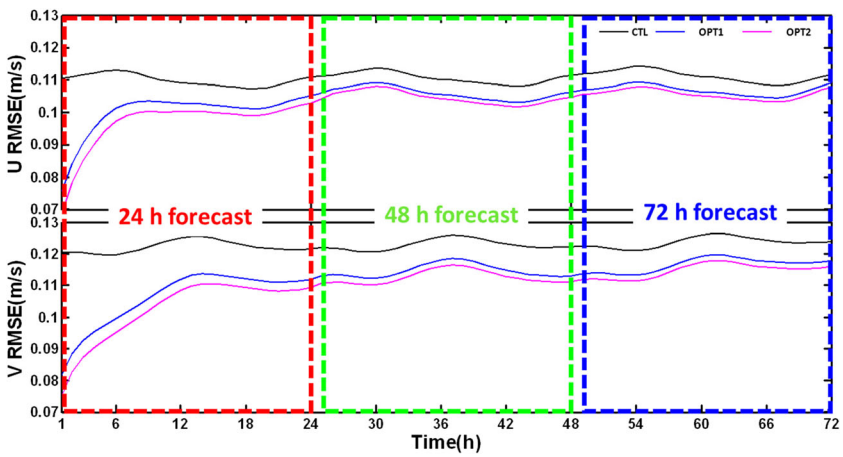

Fig. 14 The RMSE of U and V from the forecast results as a function of the forecast leading time. The CTL represents the experiment without data assimilation, OPT1 for the assimilate observations of the network OPT1, and OPT2 for the assimilate observations of the network OPT2

The coastal ocean model for the Gulf of Thailand based on FVCOM and the related data assimilation scheme had been designed to assimilate observed surface currents. The real forecast experiments show that the observation from the radars could improve the forecast in this region but observing network needs to be optimized for further improvement. Some experiments have been carried out to evaluate the impacts from the observations by the radars in different regions. The experimental results showed that the coastal high frequency radar surface current observation system plays a quite positive role in improving the current simulation in the whole research domain, although the observation only covers small parts of this area. The existing observation system is helpful for ocean circulation simulation and forecast. However, the improvement for three observation regions was quite different. The results indicated that the configuration of the existing surface current observation system in the Gulf of Thailand is not effective and a further design is required.

Based on the original observing network, the redundant and inefficient observation region in original system was discarded and some new observation regions were added in the areas where the degree of improvement was relatively smaller. This scheme manually adjusted according the evaluation of the assimilation performance. Following the way used in Sakov and Oke (2008), an objective scheme has been obtained. Numerical experiments based on these two observing schemes and the results show that the objective scheme-based ensemble Kalman filter was more reasonable than the manual scheme in improving the simulation of both the surface currents and subsurface currents. As for the forecast skills of 24, 48, and 72 h, the forecast error from the objective scheme was much lower than that of manual scheme. In general, the optimal scheme for observing network based on data assimilation is much superior to the manual scheme that based on the evaluation of current observing networks in the Gulf of Thailand. The distributions of the optimal network of radars from this study will provide very useful advice to the related governments or the units who want to design more observing stations in the Gulf of Thailand.

Although the observing scheme based on data assimilation is much superior, there are still some treatments should be improved. First, when considering the system errors in this region, the errors in different locations have the same weight. In fact, for a forecast system, people will be more interested in the regions where human activities are more frequent. Mostly, the region near the land is more important than the inner regions. Putting more weight on the active regions will obtain some different observing scheme and this will make the forecast more accurate in the human active regions than the one from this study. On the other hand, since the radar stations are on the land, the optimal observing locations far from land should be given up. A better way to do is that only considering the locations where the radar stations are possible during the procedure of finding the optimal observing locations. This will also reduce the computation coast in numerical experiments. Furthermore, the regions where new radar stations advised in this study are not belong to one country, more international cooperation to do the observing in the Gulf of Thailand will improve the forecast skills more efficiently.

Acknowledgements The authors would like to thank Dr. Somkiat Khokiattiwong from PMBC for providing the near-shore water depth, monthly averaged runoff amount of rivers around the Gulf of Thailand, and surface current observations by high frequency ground wave radar and also to the two anonymous reviewers for their thorough examination and comments that were very useful for improving the manuscript.

Funding information The work is supported by the Public Science and Technology Research Funds Projects of Ocean (201505013), International Cooperation Project of Indo-Pacific Ocean Environment Variation and Air-Sea Interaction (GASI-IPOVAI-05 and GASI-03-IPOVAI-06), and NSFC-Shandong Joint Fund for Marine Science Research Centers (Grant No. U1406404).

References

Atlas R, Hoffman R , Ardizzone J, et al. (2009) Development of a new cross-calibrated, multi-platform (CCMP) ocean surface wind product [C]. Paper presented at AMS 13th Conference on Integrated Observing and Assimilation Systems for Atmosphere, Oceans, and Land urface (IOAS-AOLS), Phoenix, AZ

Atlas R, Hoffman RN, Ardizzone J, Leidner SM, Jusem JC, Smith DK, Gombos D (2011) A cross-calibrated, multiplatform ocean surface wind velocity product for meteorological and oceanographic applications. Bull Am Meteor Soc 92:157–174. https://doi.org/10.1175/2010BAMS2946.1

Baker N, Daley R (2000) Observation and background adjoint sensitivity in the adaptive observation-targeting problem. Q J R Meteorol Soc 126(565):1431–1454

Bergot T, Hello G, Joly A, Malardel S (1999) Adaptive observations: a feasibility study. Mon Weather Rev 127(5):743–765

Bishop C, Etherton B, Majumdar S (2001) Adaptive sampling with the ensemble transform Kalman filter. Part I: theoretical aspects. Mon Weather Rev 129(3):420–436

Bishop C, Toth Z (1999) Ensemble transformation and adaptive observations. J Atmos Sci 56(11):1748–1765

Buizza, Gelaro R, Molteni R, et al (1995) Predictability studies with high resolution singular vectors. Ecmwf

Chen C, Beardsley R, Cowles G (2006) An unstructured grid, finite-volume coastal ocean model: FVCOM user manual, second edition. Oceanography 19(1):78–89

Evensen G (2004) Sampling strategies and square root analysis schemes for the EnKF. Ocean Dyn 54(6):539–560

Evensen G (1994) Sequential data assimilation with a nonlinear quasi-geostrophic model using Monte Carlo methods to forecast error statistics. J Geophys Res Oceans 99(C5):10143–10162

Gelaro R, Errico R, Prive N (1999) Development of an OSSE framework for a global atmospheric data assimilation system (invited)[M]. Intelligent transportation systems architectures. Artech House, Norwood, pp 121–139

Jackson D, Keil M, Devenish B (2008) Use of Canadian quick covariances in the Met Office data assimilation system. R Meteorol Soc 134:1567–1582

Kalnay E, Kanamitsu M, Kistler R et al (1996) The NCEP/NCAR 40-year reanalysis project. Bullamermeteor Soc 77(3):437–472

Langland R, Gelaro R, Rohaly G et al (1999) Targeted observations in FASTEX: adjoint-based targeting procedures and data impact experiments in IOP17 and IOP18. Q J R Meteorol Soc 125(561):3241–3270

Masutani M, Schlatter TW, Errico RM et al (2010) Observing system simulation experiments. In: Data Assimilation, pp 647–679

Morss R, Snyder C, Emanuel K (2001) Idealized adaptive observation strategies for improving numerical weather prediction. J Atmos Sci 58(2):210–232

Palmer T, Buizza R, Molteni F et al (1994) Singular vectors and the predictability of weather and climate. Philos Trans Phys Sci Eng 348(1688):459–475

Palmer T, Gelaro R, Barkmeijer J et al (1998) Singular vectors, metrics, and adaptive observations. J Atmos Sci 55(4):633–653

Pawlowicz R, Beardsley B, Lentz S (2002) Classical tidal harmonic analysis including error estimates in MATLAB using T_TIDE. Comput Geosci 28(8):929–937

Peng S, Zeng X, Li Z (2016) A three-dimensional variational data assimilation system for the South China Sea: preliminary results from observing system simulation experiments. Ocean Dyn 66(5):737–750

Saha S, Moorthi S, Wu X et al (2012) The NCEP climate forecast system version 2. J Clim 27(6):2185–2208

Sakov P, Oke P (2008) Objective array design: application to the tropical Indian Ocean. J Atmos Ocean Technol 25(5):794–807

Saramul S, Ezer T (2014) On the dynamics of low latitude, wide and shallow coastal system: numerical simulations of the upper Gulf of Thailand. Ocean Dyn 64(4):557–571

Scott J, Wentz F, Hoffman R, et al. (2016) Improvements and advances to the cross-calibrated multi-platform (CCMP) ocean vector wind analysis (V2.0 release)[C]. AGU Ocean sciences meeting

She J, Hoyer J, Larsen J (2007) Assessment of sea surface temperature observational networks in the Baltic Sea and North Sea. J Mar Syst 65(1–4):314–335

Shi J, Yin X, Shu Q et al (2018) Evaluation on data assimilation of a global high resolution wave-tide-circulation coupled model using the tropical Pacific TAO buoy observations. Acta Oceanol Sin 37(3):8–20

Sun M, Yin X, Yang Y et al (2017) An effective method based on dynamic sampling for data assimilation in a global wave model. Ocean Dyn 67(3–4):1–17

Tomkratoke S, Sirisup S, Udomchoke V, Kanasut J (2015) Influence of resonance on tide and storm surge in the Gulf of Thailand. Cont Shelf Res 109:112–126

Weatherall P, Marks KM, Jakobsson M, Schmitt T, Tani S, Arndt JE, Rovere M, Chayes D, Ferrini V, Wigley R (2015) A new digital bathymetric model of the world's oceans. Earth Space Sci 2(8):331–345

Xue P, Chen C, Beardsley R et al (2011) Observing system simulation experiments with ensemble Kalman filters in Nantucket Sound, Massachusetts. J Geophys Res Atmos 116(C1):325–332

Yin X, Qiao F, Shu Q (2011) Using ensemble adjustment Kalman filter to assimilate Argo profiles in a global OGCM. Ocean Dyn 61(7):1017–1031